

1
2
3
4
5

MACHINING SCIENCE AND TECHNOLOGY
Vol. 6, No. 3, pp. 485–492, 2002

6 TECHNICAL REPORT

7
8
9

**ACCELERATED WEAR TESTS FOR THE
ASSESSMENT OF MACHINING MODELS
CALIBRATION DATA***

10

R. W. Ivester[†] and M. Kennedy

11
12
13
14

National Institute of Standards and Technology, Gaithersburg,
MD 20899, USA

15

ABSTRACT

16
17
18
19
20
21
22
23

This paper documents the release of the accelerated wear tests for the Assessment of Machining Models (AMM) calibration data set, including some brief background material and a summary of previously published results. Measurements and results for the accelerated wear tests are summarized and a representative plot is given. Sources of uncertainty associated with the accelerated wear test measurements are discussed. The paper closes with a brief discussion of the wear test data and the complete data files, which are available through the project web site at <http://www.nist.gov/amm/>.

AQ1

24

INTRODUCTION

25
26
27
28

This paper documents progress to date of the Assessment of Machining Models (AMM) consortium in pursuit of its goals and objectives. The consortium's primary goal is to assess the ability of machining models to make accurate predictions of the practical behavior of machining operations, and identify focus areas for future research.

*Official contribution of the National Institute of Standards and Technology; not subject to copyright in the United States.

[†]Corresponding author. Fax: (301) 975-8058; E-mail: ivester@nist.gov

30 The basic plan for achieving this goal is to build the required data sets, solicit model-
31 based predictions, compare the predictions to the data sets, and report the results. This
32 paper documents the release of the final component of the data set, the accelerated
33 wear test calibration data. Together with the already released force and temperature
34 calibration data, the raw files for the complete data set are available from the AMM
35 project web site at <http://www.nist.gov/amm/>.

36 The motivations for the AMM effort, the experimental approach, measurement
37 techniques, and preliminary results were discussed in detail at the 3rd International
38 CIRP Workshop on Modeling of Machining Operations, and published subsequently in
39 the *Journal of Machining Science and Technology*.^[1,2] Wherever possible, the details of
40 these aspects of the project are omitted for brevity. In particular, the scope of this paper
41 is limited to discussion of measurements of worn tools from the accelerated wear tests.

42 More than a century of published machining research has been driven by the
43 tremendous practical utility of machining operations and an avid scientific curiosity for
44 exploring complex physical phenomena in an applied context. Machining operations
45 subject the tool and workpiece to extremely localized and nonlinear physical phe-
46 nomena over a wide ranges of temperatures, pressures, and strain rates. Insight into the
47 nature of these physical phenomena requires painstaking research and extensive labo-
48 ratory facilities. Driven by a tremendous economic motivation,^[3] machining research
49 directed at the practical aspects of machining performance dates back to Taylor's
50 extensively detailed reports on tool life in 1906.^[4] Analytical research directed at the
51 mechanistic behavior of machining processes dates back even further to 1888^[5] when
52 Mallock presented insights into the mechanics of chip formation. In the ensuing century
53 of research, the next major period of development was in the 1930's and 1940's, when
54 Piispanen,^[6] Ernst,^[7,8] and Merchant^[9-12] placed the study of machining mechanics on
55 a solid physical and mathematical foundation.

56 In the remaining 50 years of machining research, a vast body of published literature
57 has been developed, see for example.^[13-15] See Ref. [2] for an overview and brief
58 description of some of the research most relevant to AMM. Despite a century of in-
59 formative and high quality research, the complexity of the underlying physical phenomena
60 in machining operations has hindered progress in developing a practical predictive
61 capability based on a fundamental understanding of machining operations. Success in
62 prediction of practical machining performance parameters has been limited to one or a few
63 combinations of workpiece materials, machines, and cutting tools for reasons of
64 practicality. With the introduction of new workpiece materials, improved machine ca-
65 pabilities, and new cutting tool geometries, materials, and coatings, the practical utility of
66 previous successes is reduced. The increasing pace of introduction of new materials
67 and capabilities motivates a broader approach to modeling where the influences of
68 material properties on the relationships between performance measures and process
69 parameters are known and explicitly defined. Understanding these influences would
70 enable performance prediction for new workpiece materials based on their material
71 properties and previous experience machining other materials. As a first step toward
72 independently validated predictive process models, the Assessment of Machining
73 Models effort will provide baseline measures of the capability of predictive models.

74 A detailed plan for the AMM effort, the design of the experiments for build-
75 ing the data sets, and a breakdown of measurement techniques and representative
76 results have been addressed in a prior publication.^[2] The bulk of these discussions

T1.1 **Table 1.** Process Parameters for Orthogonal Cutting Calibration (OCC) and Accelerated Wear (AW) Tests

T1.2	Test	Speed (m/min)	Feed ($\mu\text{m}/\text{rev}$)	Rake Angle
T1.3	OCC-1	200	150	-7
T1.4	OCC-2	200	150	+5
T1.5	OCC-3	200	300	-7
T1.6	OCC-4	200	300	+5
T1.7	OCC-5 (AW)	300	150	-7
T1.8	OCC-6	300	150	+5
T1.9	OCC-7	300	300	-7
T1.10	OCC-8	300	300	+5

77 is omitted, but brief overviews of relevant sections are included to provide context
78 where appropriate.

79

EXPERIMENTAL PROCEDURE

80 The cutting tests for the AMM orthogonal cutting calibration and validation data
81 sets were performed in accordance with the experimental procedures and measurement
82 techniques, as described in Refs. [1,2]. For the accelerated wear tests, the same pro-
83 cedures and techniques were employed, with appropriate additions for characterizing
84 the state of wear of the tool, also described in Refs. [1,2]. Detailed descriptions of the
85 process, tooling, and workpiece material selections, as well as metallurgical, chemical,
86 mechanical, and ultrasonic examinations of the workpiece material are included in
87 Refs. [1,2]. The process parameters for the orthogonal cutting calibration (OCC), and
88 accelerated wear (AW) tests are given in Table 1. As shown in the table, an accelerated
89 wear test was performed for one of eight combinations of orthogonal cutting calibration
90 test parameters, OCC-5. Each of four laboratories conducted four repetitions of OCC-5.
91 Of these 16 tests, 7 were performed with uncoated inserts and 9 with coated inserts.
92

T1

93

MEASUREMENT PROCEDURE AND RESULTS

94 Wear measurements were conducted according to ISO 3685. The following
95 methods of measuring wear patterns were investigated and compared: 1) air bearing
96 linearly variable differential transducer (LVDT) (crater depth); 2) white-light inter-
97 ferometer (500 micrometer vertical travel with 10 nm resolution and 5 mm by 5 mm
98 field of view with a 320×256 pixel array); 3) optical microscope (50 cm vertical travel
99 with 1 micrometer resolution and varying field of view at $50\times$, $100\times$, and $200\times$
100 magnifications); and 4) scanning electron microscope. In general, the coated and
101 uncoated inserts exhibited dramatically different wear patterns. The SEM was used
102 primarily for qualitative imaging of worn tools.

103 The uncoated inserts formed craters on the rake faces and wear lands on the flank
104 faces. For the seven uncoated inserts, crater depth was measured with the 1) LVDT,

T2.1 **Table 2.** Measurements of Wear for Uncoated Inserts

T2.2	AWT Number	Length of Cut (m)	LVDT (μm)	Opt. Mic. (μm)	Interferogram (μm)	Avg. Land Width (mm)
T2.3	1	25.9	133	130	132.5	0.180
T2.4	2	25.6	135	126.04	133.4	0.182
T2.5	3	32	145	142.71	148.7	0.240
T2.6	4	28.8	150	135.42	153	0.250
T2.7	5	28.8	152	146.87	160	0.256
T2.8	6	32	134	142.71	137	0.220
T2.9	7	32	144	141.67	144	0.252

105 2) the interferometer, and 3) the optical microscope, and width of the flank wear land
 106 with the optical microscope, as given in Table 2. The $\pm 2\sigma$ expanded uncertainties^[16]
 107 for crater depth measurements with (1), (2), and (3) are $\pm 3 \mu\text{m}$, $\pm 1.5 \mu\text{m}$, and $\pm 2 \mu\text{m}$,
 108 respectively. The expanded uncertainty for width of wear land measurements with the
 109 optical microscope is $\pm 3.5 \mu\text{m}$.

110 For the nine coated inserts, the dominant wear patterns were notches and flank
 111 wear. Optical micrographs of the rake and flank faces at $200\times$ magnification were
 112 used to measure the widths and lengths of notches and width of the flank wear land,
 113 as given in Table 3. The $\pm 2\sigma$ expanded uncertainties for these widths and lengths is
 114 $\pm 5 \mu\text{m}$.

115 The above expanded uncertainties were calculated by taking the square root of
 116 the sum of the squares (summation in quadrature) of a series of uncertainty terms
 117 associated with various specific uncertainty sources of two types, systematic errors and
 118 statistical repeatability. For each of the measurement types, the appropriate sources of
 119 systematic uncertainty were selected based on the capabilities and limitations of the
 120 measurement equipment and the measurement technique.

121 For the LVDT measurements, the insert was cleaned and placed directly on a flat
 122 granite work surface, and the 0.1 mm radius probe tip was referenced from a flat
 123 unused portion of the cutting insert near the crater. The probe tip was fixed in the x-y

T3.1 **Table 3.** Measurements of Wear for Coated Inserts

T3.2	AWT Number	Length of Cut (m)	Average Land Width (mm)	Notch Width (mm)
T3.3	1	29	0.043	n.a.
T3.4	2	32	0.045	0.166
T3.5	3	39	0.050	0.224
T3.6	4	28	0.045	n.a.
T3.7	5	25	0.043	0.317
T3.8	6	32	0.063	0.781
T3.9	7	39	0.080	1.300
T3.10	8	32	0.045	0.128
T3.11	9	32	0.050	0.139

124 directions, and the insert was moved relative to the probe and granite surface. Veri-
125 fication that the granite and insert surfaces are adequately level and parallel stems from
126 moving the insert so that the probe tip contacts at various locations around the
127 periphery of the crater. In general, the LVDT measurement changed by $\pm 1 \mu\text{m}$ around
128 the periphery of the crater. The insert was then moved so that the probe tip contacted at
129 the bottom of the crater by adjusting the insert position in x - y until the LVDT
130 measurement was maximized. Since the bottom of the crater is much flatter than the
131 probe tip, the radius of curvature of the probe tip does not contribute significantly to
132 the uncertainty after summation in quadrature. Similarly, variation in the surface texture
133 geometry was on the order of $0.1 \mu\text{m}$; it also does not contribute significantly to the
134 uncertainty. The dominant contributing factors are the $\pm 2 \mu\text{m}$ associated with the
135 variation of measurements around the periphery of the crater, and $\pm 2 \mu\text{m}$ for manually
136 locating the insert at the appropriate x - y location so that the probe tip contacts at the
137 bottom of the crater. The resulting quadrature summation is rounded up from 2.8 to 3
138 to provide an accounting of the smaller contributing factors.

139 For the interferometer measurements of crater depth, the dominant factors
140 contributing to the uncertainty are associated with the spacing between pixels in the
141 resulting interferogram, and the associated change in depth. With a 5 mm field of view
142 and a 320×240 pixel array, the pixels are approximately $15.6 \mu\text{m}$ by $20.8 \mu\text{m}$ in the
143 x - y plane, and the change in height of the crater surface over this distance is
144 approximately $\pm 1 \mu\text{m}$ near the bottom of the crater. The 10 nm vertical resolution of
145 the interferometer is then a negligible factor in the uncertainty. There is also a $\pm 1 \mu\text{m}$
146 uncertainty associated with the flatness/levelness of the reference surface (the original
147 "flat" face of the insert).

148 For the optical microscope measurements of crater depth, the insert was placed
149 on a leveled x - y - z micrometer stage under the microscope. The microscope was set at
150 $400 \times$ magnification, which results in a depth of focus of $\pm 1 \mu\text{m}$ in the z direction.
151 The insert was then moved using the x - y - z stage such that the edge of the crater is
152 focused in the center of the field of view. By moving around the periphery of the crater
153 in x - y , and then checking the focus by moving the z stage up and down, the flatness/
154 levelness of the border of the crater was found to be $\pm 1 \mu\text{m}$. Finally, the insert was
155 moved to the center of the crater in x - y , and adjusted in z until the bottom of the
156 crater came into focus. Finally, the insert was moved in x - y until the focus location
157 occurred at a minimum z value. The change in the z -value between the bottom of the
158 crater and the periphery is then the crater depth. The primary sources of uncertainty
159 associated with this measurement stem from the $\pm 1 \mu\text{m}$ focus depth at both the crater
160 bottom and periphery. In each case, the actual surface location that is in focus may be
161 anywhere within this $\pm 1 \mu\text{m}$ range, so the total uncertainty is then the summation in
162 quadrature of the $\pm 1 \mu\text{m}$ for both points, or $\pm 1.4 \mu\text{m}$ total.

163 For the measurements of wear land width and notch width, the relevant feature
164 was leveled with respect to the microscope image plane, so that any region of the
165 surface that is within focus is flat to within the depth of focus of the microscope at that
166 magnification. For notch width, this would be the periphery of the notch. For the land
167 width, the region is the land itself. An additional source of uncertainty in the width of
168 the feature in question stems from the pixel spacing in the digitized image from the
169 microscope. Features are sized according to the number of pixels in a line that are
170 deemed to be in focus, so the uncertainty of ± 1 pixel spacing must be included for the

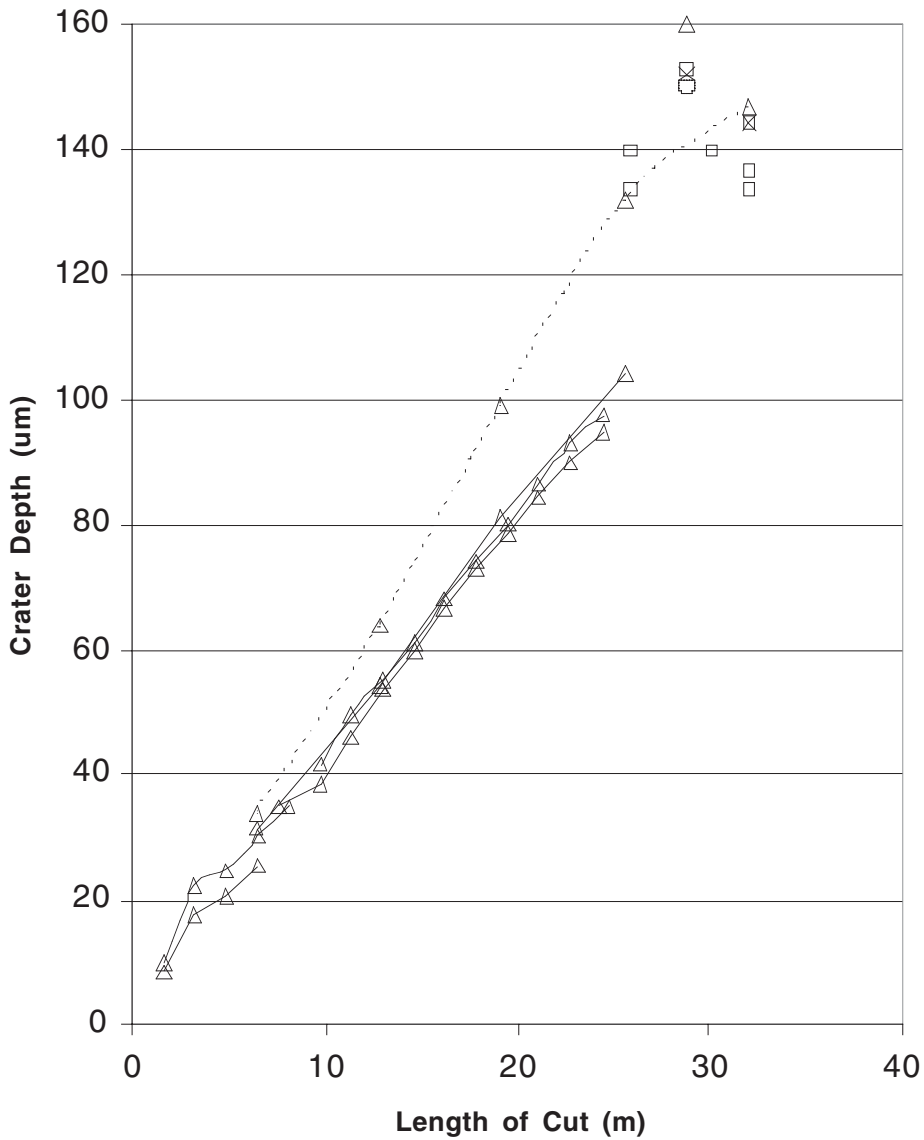
Wear Progression for Uncoated Insert

Figure 1. Measured crater wear progressions in orthogonal wear tests showing white light interferometer measurements (triangles), LVDT measurements (squares) and optical microscope (crosses).

171 location of each side of the feature. The total expanded uncertainties for land/notch
172 widths at $200\times$ and $400\times$ are the summation in quadrature of two pixel spacings
173 ($2\ \mu\text{m}$ for $100\times$ and $1\ \mu\text{m}$ for $200\times$) and the depth of focus ($\pm 2\ \mu\text{m}$ for $200\times$ and ± 1
174 μm for $400\times$), yielding approximately $\pm 3.5\ \mu\text{m}$ for $200\times$ and $\pm 1.8\ \mu\text{m}$ for $400\times$.

175 Figure 1 shows progressions of crater wear depth for different lengths of cut. For F1
176 two of the tests with uncoated inserts, cutting was stopped every 1.6 m length of cut
177 (5 mm of tube length) and the crater was measured with an optical microscope, an
178 LVDT air bearing indicator, and a white-light interferometer. The wear progressions
179 are for nominally identical cutting conditions and demonstrate a high degree of repeat-
180 ability in the wear progression when performed on a single machine. The agreement
181 between measurements of wear formations for nominally identical experiments
182 performed at different labs is reasonable given the complete change of dynamic and
183 static behaviors associated with differences in machine tools. The squares represent
184 LVDT measurements of peak crater depth. The triangles represent measurements of
185 peak crater depth from the interferometer. The crosses represent measurements of peak
186 crater depth from the optical microscope. Overall, the agreement between the different
187 measurement techniques is within the bounds defined by the expanded uncertainties.

188 The inclusion of expanded uncertainties in this paper is intended to assist in
189 proper interpretation of the data provided. More importantly, it is also a guideline for
190 interpretation of the raw data that these statistics are computed from. The inter-
191 ferograms and optical micrographs for all of these tests are available through the
192 project web site, so the interested reader can peruse the data files with a meaningful
193 guide as to the significance of trends in the data in light of the uncertainty analysis
194 provided. This is of particular importance to researchers interested in participating in
195 the AMM effort by contributing predictions of the validation data set based on the
196 calibration data discussed here.

197

198

SUMMARY

199 This paper documents the release of the accelerated wear tests for the Assessment
200 of Machining Models (AMM) calibration data set, including background material and a
201 summary of previously published results. Measurements and results for the accelerated
202 wear tests are summarized and a representative plot is given. Sources of uncertainty
203 associated with the accelerated wear test measurements are discussed. The paper closes
204 with a brief discussion of the wear test data and the complete data files, which are
205 available through the project web site.
206

207

ACKNOWLEDGMENTS

208 First, I would like to thank the AMM consortium members, Robin Stevenson,
209 Shiva Kalidas, Jeffrey Thiele, Rich Furness, and Shounak Athavale, who have provided
210 vital contributions by helping to design, plan, and conduct this effort. Also, I would
211 like to take this opportunity to thank the many other people who have contributed to
212 the development and implementation of this effort, including Matthew Davies, Ranajit
213 Ghosh, Ming Leu, Vivek Chandrasekharan, Bob Polvani, Tony Schmitz, Robyn Smith,

214 and Dieter Ebner. This work was supported in part by National Science Foundation
215 Grant Number 9909130.

216

REFERENCES

- 217 1. Ivester, R.; Kennedy, M.; Davies, M.; Stevenson, R.; Thiele, J.; Furness, R.;
218 Athavale, S. Assessment of Machining Models: Progress Report. In *Proceedings of*
219 *the 3rd CIRP International Workshop on Modeling of Machining Operations,*
220 *Melbourne, Australia, 2000.*
- 221 2. Ivester, R.; Kennedy, M.; Davies, M.; Stevenson, R.; Thiele, J.; Furness, R.;
222 Athavale, S. Assessment of machining models: Progress report. *J. Mach. Sci.*
223 *Technol.* **2000**, *4* (3), 511–538.
- 224 3. Merchant, E. *Proceedings of the CIRP International Workshop on Modeling of*
225 *Machining Operations, Atlanta, GA, USA; 1998.*
- 226 4. Taylor, F.W. *Trans. ASME* **1906**, *28*, 70–350. AQ2
- 227 5. Mallock, A. *Proc. R. Soc. London* **1881**, *33*, 127–139.
- 228 6. Piispanen, V. *Tek. Aihakak.* **1937**, *27*, 315.
- 229 7. Ernst, H. Physics of Metal Cutting. In *Machining of Metals*; American Society of
230 Metals, 1938; 1–34.
- 231 8. Ernst, H.; Merchant, M.E. *Trans. ASME* **1941**, *29*, 299.
- 232 9. Merchant, M.E. *J. Appl. Mech* **1944**, *11*, A168–A175.
- 233 10. Merchant, M.E. *Trans. ASME* **1945**, *66*, A65–A71.
- 234 11. Merchant, M.E. *J. App. Phys.* **1945**, *16*, 267.
- 235 12. Merchant, M.E. *J. App. Phys.* **1945**, *16*, 318.
- 236 13. Shaw, M.C. *Metal Cutting Principals*; Oxford Press: Oxford, UK, 1984.
- 237 14. Trent. *Metal Cutting*; Butterworth-Heinemann: Oxford, 1991. AQ3
- 238 15. Komanduri, R. *Appl. Mech. Rev.* **1993**, *46* (3), 80–129.
- 239 16. Taylor, B.N.; Kuyatt, C.E. Guidelines for Evaluating and Expressing the
240 Uncertainty of NIST Measurement Results. In *National Institute of Standards*
241 *and Technology Technical Note (TN) 1297*; 1994.
- 242